Simulation, Fabrication, and Performance Comparison of a GPS Antenna with Radome on the Roof of an Automobile

M. Tecpoyotl-Torres and J. G. Vera-Dimas

Centro de Investigación en Ingeniería y Ciencias Aplicadas, (CIICAp)
Universidad Autónoma del Estado de Morelos (UAEM), Cuernavaca, Mor. 62209, México
tecpoyotl@uaem.mx, gvera@uaem.mx

Abstract ─ In this work, a circularly polarized patch antenna, designed to operate at 1.57 GHz, is used for reception of GPS signals. Its analysis is carried out at first, by means of simulation, considering the following cases: antenna without radome and antenna with acrylic radome. It is shown that the radome produces a distortion of the electric field components. The antenna performance, with radome, was analyzed on several locations on the automobile, considering the effect of the complete chassis. Two cases of basic, a simplified and a more simplified advanced car models (BCM, SACM, and MSACM) were used in order to analyze the influence of chassis shape. Simulations demonstrate that the best location of the antenna is on the roof. Fabrication, experimental and practical tests are also presented. The performance analysis of the developed antenna, using it as a replacement one, is realized using a Garmin GPS and a GPS kit.

Index Terms – Axial ratio, car model, circular polarization, patch antennas, and Rogers RT/Duroid 5880.

I. INTRODUCTION

The evolution of the automobiles has answered several demands of the users. Especially in wireless communication systems, the necessity of aesthetic and efficiency has determined several proposals of antenna designed considering different types of materials and geometries. The location of the antennas constitutes also a very interesting analysis problem [1, 2].

The automotive sector has been interested in development and implementation of navigation systems [3], which are considered as one of the most important equipment of the automobile. They are formed by a global position system (GPS), with a pre-charged base of maps and highways in order to locate the vehicle. With the increase in automobile usage, accurately determining its location has become one of the growing priorities. The main advantages of the navigation systems are reduction in the time of journey, in consumption of combustible, and in the emission of contaminant gases [4]. Other application of the GPS technology is automatic location of vehicles (AVL) [5-6], as the medium to determine the geographic position of the vehicle and to transmit this information to the place where it can be used and exploited. This tool is extremely useful to the management of fleets of service vehicles, emergencies, construction, public transportation, recovery stolen vehicles, and public security [7].

The GPS satellites, often referred as SVs (for space vehicles), transmit on two frequencies in the L-band, designated as Link 1 (L1) at 1575.42 MHz, and Link 2 (L2) at 1227.60 MHz. The L1 band contains a civil signal and an encrypted military signal, and is available for commercial uses [8]; the L2 band contains another encrypted signal for military use [9, 10]. In Mexico the corresponding frequency segment is referred as 17, radio-navigation by satellite (space-earth, space-space) [11]. For the purposes of this paper, only the civil signal on L1 is of interest. Placement of a GPS antenna is critical; the roof of the automobile is considered as the most effective location to place an antenna, in terms of GPS signal reception, as it was experimentally demonstrated in [12]. The GPS antenna design has received special attention. Toyota central R&D laboratories of Japan has developed an antenna for

Submitted On: Jun. 25, 2012
Accepted On: Apr. 24, 2013

installation on the roof of an automobile [2]. They have used a dual-feed, stub loaded single patch to achieve circular polarization at the two frequencies of the satellite.

Motorola, one of the leading manufacturers of automotive GPS systems, recommends the placement of the GPS antennas at the roof, roofline or trunk [13]. On the other hand, the antenna radomes have received special attention, not only on the materials used, but also in shapes. Additionally, several companies found a niche market in the commercialization of navigation systems, because austere vehicles do not account with them [14]. The antennas contribute greatly to the total operation of the navigation systems, and they can be designed in accordance to the aesthetics and the requirements of the vehicle, to obtain totally personalized prototypes.

The satellite systems NAVSTAR-GPS [8] and Galileo [15] transmit right-hand circularly polarized signal (RHCP). Galileo provides 10 navigation signals with RHCP. Due to the antenna reciprocity, the receptor antenna must be also RCP. The main advantage of CP is that regardless of receiver orientation, it will receive a component of signal [16]. Antennas, commonly used for circular polarization, are based on corner-truncated square microstrips [17], and on square or circular patches with one or two feed points [2]. A circular polarization can, also, be obtained from a single-point square or circular patch.

In this research, the design of a circular patch antenna for GPS is realized. The interest is focused on the simulation of the antenna, due to the benefits to know the performance of the complete system. The software used for simulations is FEKO. The circular antenna is designed considering a unique feed point and a substrate of RT/Duroid 5880. Three car models, basic, simplified and more simplified advanced car models (BCM, SACM, and MSACM) were used in order to analyze also the influence of the chassis shape on simulation. In [18], two automobile similar models can be found, using monopole and multi-element antennas. The analysis of a multi-functional antenna on the automobile are carried-out in [19], using four simulation cases.

The content of this paper is organized as follows. In section II, the principles of the circular antenna design are mentioned. The simulations considering the antenna without and with acrylic radome are shown in sections III and IV. Simulations of the antenna considering three car models are presented in section V. In section VI, the fabrication process is briefly described. The simulated, experimental, and practical results are presented in section VII and discussed in section VIII. Finally, in section IX, some concluding remarks are given.

II. INDIVIDUAL PATCH ANTENNA DESIGN

A simple approximation [20] is used for the design of the circular patch antenna (CPA),

$$r = \frac{\lambda_g}{\pi}, \quad \text{with} \quad \lambda_g = \frac{c}{f_0\sqrt{\varepsilon_{reff}}}, \qquad (1)$$

where r is the patch radius, λ_g is the group wavelength, c is the speed of light in free space, ε_r is the dielectric permittivity and f_0 is the operation frequency. The length of the square ground plane side is equal to the resonator patch diameter plus $6h$, where h is the substrate thickness [21]. Equation (1) is very similar to the one used for ring resonators [22]. The calculated antenna sizes of the antenna using RT/Duroid 5880 with a thickness of 3.17 mm are: patch radio, 4.19 cm, and length of the square substrate, 10.28 cm.

Coaxial type feed is used. The location of the feed point is determined in accordance to the impedance matching. Typically the input impedance of a GPS receiver is 50 ohms [8]. The simulation of the electric far field allows us to adjust the feed point location, considering the antenna impedance as a main condition. In this case, the feed point is located near to the edge of the antenna.

III. SIMULATION OF THE INDIVIDUAL PATCH ANTENNA DESIGN

Two cases were analyzed: linear and circular polarization (Fig. 1). To observe the performance of the antenna on the circular polarization, it is not necessary to modify the established values of the antenna, it is enough to select in the main menu, the component, and the values, considering the scale that we want to observe. With the selection of circular polarization, Fig. 1 (b) was obtained. The gain values are presented in Table 1. As it can be observed, the differences between linear and circular polarization values are as expected.

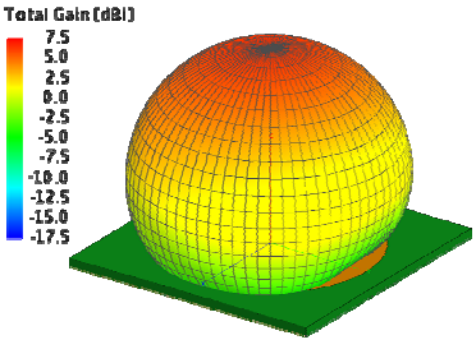

(a)

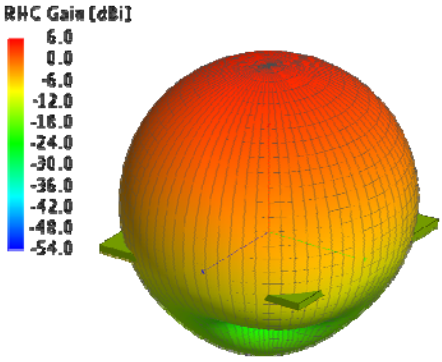

(b)

Fig. 1. Gain of the CPA considering (a) linear and (b) circular polarizations.

IV. SIMULATION OF THE ANTENNA WITH RADOME

After designing the patch antenna, it is also important to design the radome, because it prevents the early physical deterioration of the antenna and the copper oxidation, which affects lightly the performance of the antenna. It also allows easy manipulation. As a first approximation, a simple radome design of low cost, which does not affect the radiation pattern of the antenna, was chosen. Acrylic was used to implement the radome, with a thickness of 4.7 mm, due to its availability in the market. ABS (Acrylonitrile-Butadiene-Styrene) is widely used for protective housing for electronic equipment and computers, but it is more difficult to obtain and to manipulate for us. In [23], it is shown the effect of various materials on the radiation pattern of an antenna. In Fig. 2, top and cross section views of the square radome are presented. The values of the antenna gain with radome under linear and circular polarization, shown in Table 1, are slightly bigger compared to the values obtained without the radome.

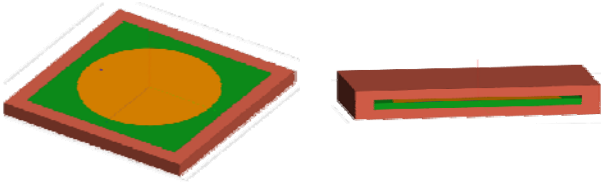

(a) (b)

Fig. 2. (a) Top and (b) cross section view of the radome containing the CPA.

Table 1: Antenna gain values.

Antenna	Gain (dB)
Without Acrylic RHC	3.957
Without Acrylic LP	6.938
With Acrylic RHC	4.198
With Acrylic LP	6.947

Simulation results of the antenna gain with acrylic radome, considering linear and circular polarization are presented in Fig. 3. The axial ratio with and without radome is shown in Fig. 4. As it can be noted, the presence of the radome produces a distortion of the electric field components.

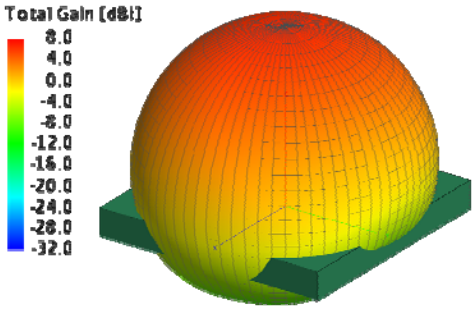

(a)

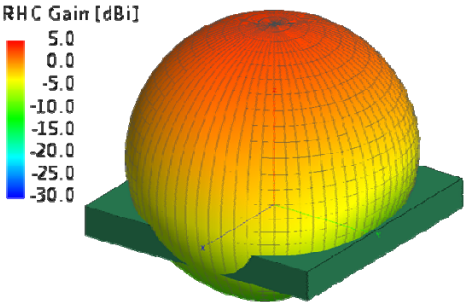

(b)

Fig. 3. 3D radiation pattern of the CPA inside the acrylic radome, with a) linear and b) circular polarizations.

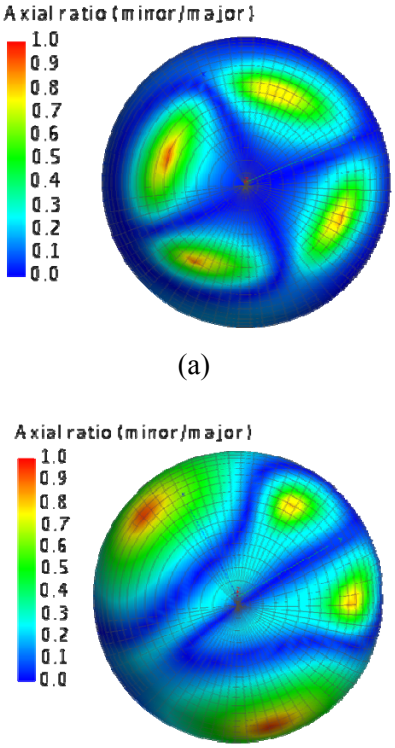

Fig. 4. Axial ratio of the antenna (a) with out and (b) with radome.

V. SIMULATION OF THE ANTENNA WITH RADOME, CONSIDERING THREE CAR MODELS

A. With a basic car model (BCM)

With the aim of observing the performance of the CPA in a more real environment, the antenna was placed on the roof of a vehicle chassis. We use a 3D drawing software that allow us to export the corresponding design in a file with extension *.x_t (parasolid files), which can be imported by CADFEKO, and after that, to realize the simulation of the complete system. The implemented car design only consists of metal layers; without doors, and other not relevant details, such as crystals, because the antenna is not closely interacting with any of them.

In order to analyze the effect of the car sizes on the antenna performance, a BCM was implemented, under two different cases (Tables 2 and 3).

Table 2: Sizes of BCMs.

BCM Features	Length (m)	Width (m)	Height (m)
Small size	4.1	1.4	1.07
Real size	4.18	1.77	1.08

Table 3: Roof sizes of BCMs.

Roof Features	Length (m)	Width (m)	Height (mm)
Small BCM	1	1.2	0.1
Real sizes BCM	1	1.6	0.1

With the vehicle design, the next step is implementing both the antenna system, and the metallic chassis in CADFEKO. In the corresponding simulations, the antenna was located on different places on the chassis (Fig. 5). The radiation patterns of the antenna gain with circular polarization considering the BCMs described in Table 2, are shown in Fig. 6. The gain values are shown in Table 4, where it can be observed that their gain values are very similar. As the gain difference between the two analyzed cases is minimal, it is possible to use any of the BCMs. We chose real size BCM in the following sections.

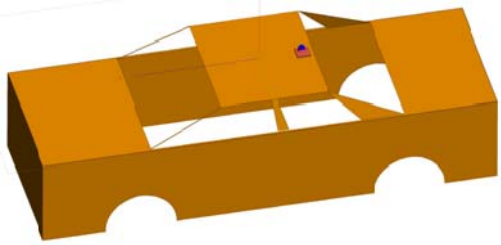

Fig. 5. View of the BCM system implemented in CADFEKO, with the patch antenna and with radome, located on the rear part of the roof.

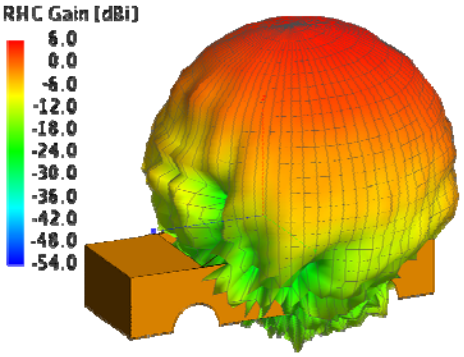

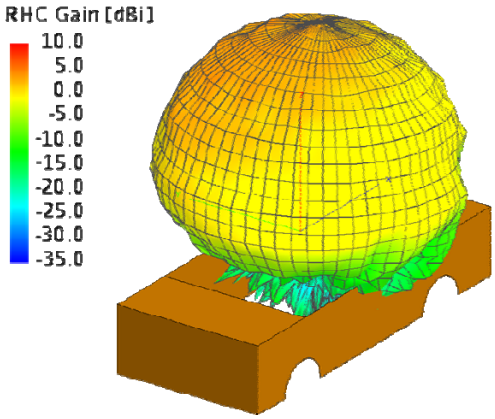

(b)

Fig. 6. Gain pattern of the CPA with acrylic radome, on the rear part of the roof of the vehicle chassis, with (a) small and (b) real size BCM.

B. With a simplified and a more simplified advanced car models (SACM and MSACM).

The model cars correspond to an AUDI R8 [24]. Due to computer limitations, we simulate a SACM (Fig. 7). The maximum width is of 1.96 m, maximum length of 4.6 m and a height of 1.09 m. The roof has a maximum and a minimum width of 1.33 m and 1.19 cm, respectively; and a maximum and a minimum length of 1.48 m and 1.28 m, respectively. The obtained gain values considering a SACM with the antenna located on several places are given in Table 5. Simulation results on the central part of the roof are shown in Fig. 8.

An MSACM was also implemented (Fig. 9). The gain when the antenna is on the central part of the roof is shown in Fig. 10, using MSACM. A summary of the gain values in other locations are also given in Table 5. In both models, the biggest gain value corresponds to the antenna located on the center of the roof.

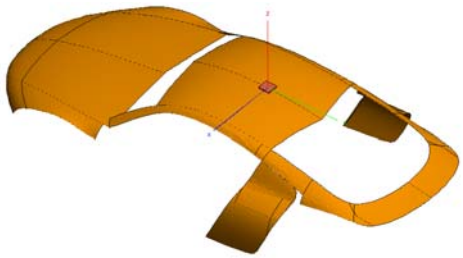

Fig. 7. SACM implemented in CADFEKO, based on an AUDI R8, with the antenna located on the central part of the roof.

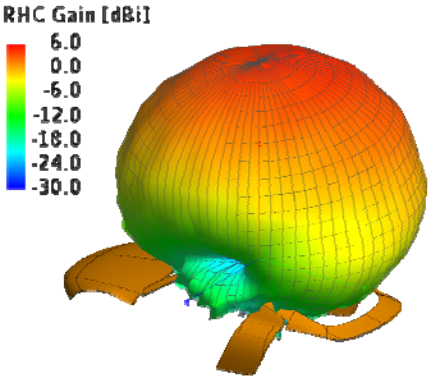

Fig. 8. Gain of the GPS antenna located on the center of the roof using SACM.

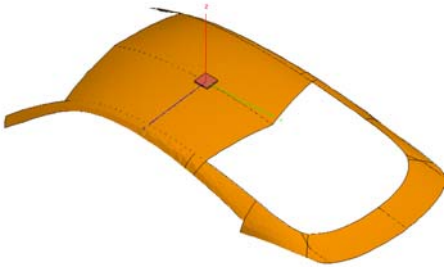

Fig. 9. View of the MSACM implemented, with the antenna located on the central part of the roof, in CADFEKO.

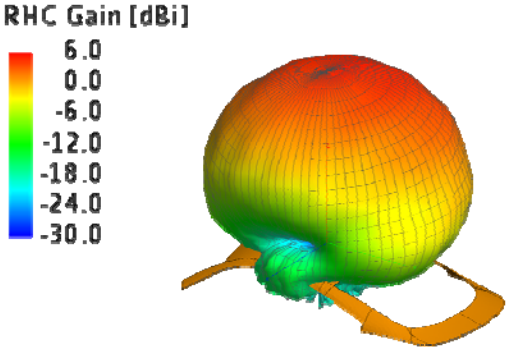

Fig. 10. Gain of the GPS antenna located on the center of the roof using MSACM.

Table 5: Gain values considering different locations of the antenna.

Position SACM	**Gain (dB)**	**Position MSACM**	**Gain (dB)**
Center	4.51	Center	4.76
Frontal	4.43	Frontal	4.7
Rear	4.4	Rear	4.44
On the trunk	4.26	On the trunk	4.34

VI. FABRICATION PROCESS

The antenna was fabricated using a PROTOMAT S-42 machine. After pattern transfer and drilling for the feeding point, the welding of the required connectors is realized (Fig. 10 (a)). For the laboratory tests, BNC female connectors of 50 Ohms to match the antenna with the experimental equipment were used. The soldering points are shown in Fig. 11. Unfortunately, the undesirable effects on the vertical profile are consequences of this feed type, which produce spurious feed radiation and poor polarization purity [2]. For experimental tests, a female MCX connector of 50 Ohms was used to couple the antenna to the GPS development kit, in order to compare its performance with the original antenna of the kit (Fig. 12) and Garmin GPS. The experimental set up is shown in Fig. 13.

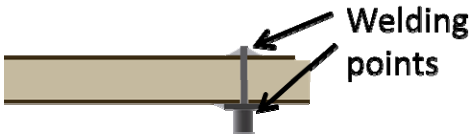

Fig. 11. Transversal section of the antenna with coaxial connector.

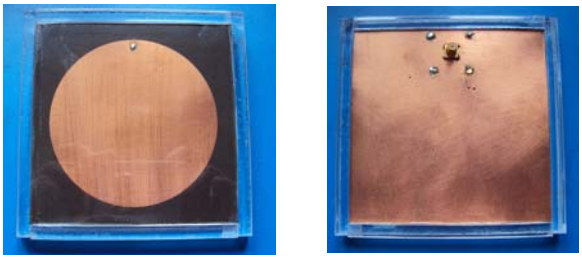

(a) (b)

Fig. 12. Front (a) and rear view (b) of the CPA with acrylic radome.

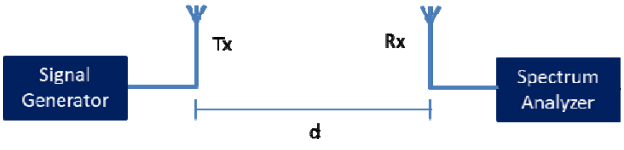

Fig. 13. Experimental set-up.

Distance d is at least of 15 cm, since the calculation of the corresponding radio of far field $\left(R > 0.62\sqrt{D^2/\lambda}\right)$, where D is the biggest size of the antenna and λ is the corresponding wavelength [25].

VII. RESULTS

A. Simulation results

In Table 6, a summary of the gain values of the antenna simulated with radome, considering the cases of sections III and IV are given.

Table 6: Gain of the circular polarization of the antenna with different car models.

Antenna location	Model	Gain (dB)
Front part, roof	BCM	5.169
Rear part, roof	BCM	5.169
Central part, roof	BCM	4.854
Central part, roof	MSACM	4.76
On trunk	MSACM	4.7
Central part, roof	SACM	4.51
On trunk	BCM	4.51
Front part, roof	MSACM	4.44
Front part, roof	SACM	4.43
Rear part, roof	SACM	4.4
Rear part, roof	MSACM	4.34
On trunk	SACM	4.26

Table 6 shows the gain values in descending order. In the BCM, the simulation results show a bigger gain values at the front and rear part of the roof. This fact can be attributed to the high symmetry in the car geometry. In the case of the antenna located at the front part of the roof in the MSACM and SACM values are very near, the same happen for the rear part. On the trunk in the MSACM, the values are almost as high as the case of the central part of the roof. The simulation of the S21 parameter of the antenna with acrylic radome is shown in Fig. 14.

B. Experimental results

The transmission-reception tests were realized using a signal synthesized generator and a spectrum analyzer (AGILENT 83732B and 8563EC, respectively). The frequency range from 1.3 GHz up to 1.8 GHz was considered to observe the antenna behavior using a constant power generated by the transmitter. The antenna separation was of 15 cm. In Fig. 14, the received power is also shown.

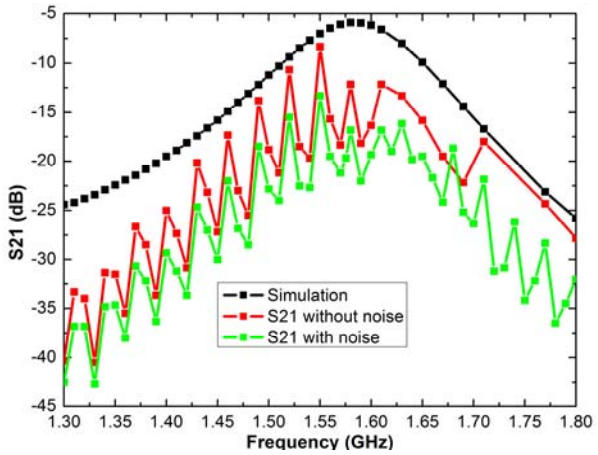

Fig. 14. Simulated and experimental S21 parameter values.

The oscillations could be attributed to the use of the connection converters to couple the laboratory equipment, and especially by the noise given by the coaxial cable.

C. Practical results

For the test of the antenna prototype as a replacement antenna, a GPS development kit was used (Fig. 15), which accounts with a GPS development card (ER-102-J, SiRF Star-II), and the NMEAgent data (this software shows the current location).

Fig. 15. GPS kit with (a) its original antenna and (b) with the replacement antenna.

The response of the antenna prototype with circular polarization can be analyzed in this case. Three measurement points were established at CIICAp parking (Fig. 16, and Table 7). Results are also compared with a Garmin GPS. Figure 17 shows the measurements trends. It can be noted, that the kit with replacement antenna provides the nearest values to the Garmin GPS measurements.

Fig. 16. Three measurement points at CIICAp parking.

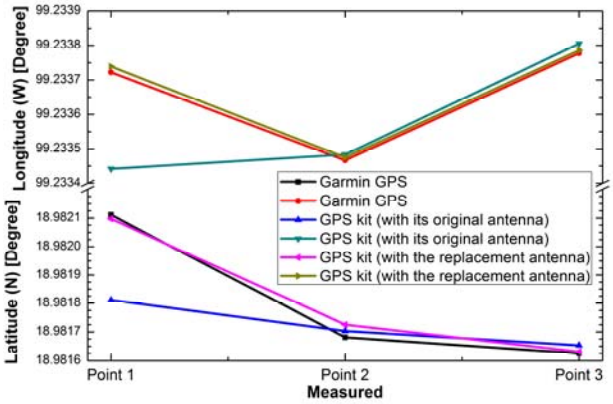

Fig. 17. Plot of points shown in Table 7.

Table 7: Measured position at 3 points in CIICAp parking.

With Garmin GPS		
Location	**Latitude (N)**	**Longitude (W)**
Point 1	18°58′5**5.6**′′	99°14′**1.4**′′
Point 2	18°58′54.**05**′′	99°14′**0.48**′′
Point 3	18°58′53.**85**′′	99°14′1.**6**′′
With GPS kit (with its original antenna)		
Point 1	18°58′5**4.52**′′	99°14′**0.39**′′
Point 2	18°58′54.**13**′′	99°14′**0.54**′′
Point 3	18°58′53.**95**′′	99°14′1.**7**′′
With GPS kit (with the replacement antenna)		
Point 1	18°58′5**5.55**′′	99°14′**1.46**′′
Point 2	18°58′54.**21**′′	99°14′**0.51**
Point 3	18°58′53.**87**′′	99°14′1.**63**′′

For the test of the antenna prototype in movement, the antenna was located on the rear roof of a Cavalier car model 95, using it as a

replacement antenna for the GPS kit (Fig. 18). The trajectory is shown in Fig. 19, and the measurement positions are points marked with arrows. The collected data are given in Table 8.

Fig. 18. Antenna location on the automobile roof.

Table 8: Measured position of several points on the university circuit.

Location	Latitude (N)	Longitude (W)
4	18°58'50.52"	99°14'2.35"
5	18°58'50.25"	99°14'5.45"
6	18°58'44.05"	99°14'9.68"
7	18°58'48.64"	99°14'14.87"
8	18°58'53.03"	99°14'21.27"
9	18°58'55.65"	99°14'25.59"
10	18°58'59.95"	99°14'19.08"
11	18°58'59.16"	99°14'12.13"
12	18°58'57.51"	99°14'5.12"

Fig. 19. Arrows indicate the place where the measurements were realized. The balloons indicate geographical locations found in Google maps.

VIII. DISCUSSION

Simulations of the antenna performance were realized considering linear and circular polarizations. For experimental tests, the available components and equipment only allow us to check the response under linear polarization. The transmission-reception test shows a peak of response in the range of GPS signals (1575.42 MHz).

It was observed in simulation of all model cases that the gain increment due to the presence of chassis is as expected without radome, with it, some variations were perceived. In the practical tests, the replacement antenna showed satisfactory results (Table 7). The measurements in fixed points, in comparison with the Garmin GPS, are nearest using the kit with the replacement antenna. In movement, as it can be observed in Fig. 19, generated using Google Maps, the measured points, except the corresponding to the CIICAp parking are located on the university circuit without invade buildings or traffic islands, which means that the measurements are useful and precise.

It is necessary to mention the following differences between the cars used in simulations and in practical tests: the model, the chassis material (in simulation, it is a perfect conductor, and in the practical tests, it was covered with black painting); and the sizes are slightly different. In experimental and practical tests, the antenna performance remains as it was expected. The symmetry influences the gain value and the pattern shape, showing in all cases a bigger gain in the central and rear part of the roof.

IX. CONCLUSIONS

Due to the presence of changes in the gain values of the antenna according to the system where it is immersed, it is desirable to perform the simulation considering the complete system elements, in order to know a more real behavior. However, it requires the combination of technological factors in order to perform these simulations and higher computer capabilities.

Surely, the antenna performance can be improved, in our BCM. This model provides a simple approximation to complex shapes. Our purpose was only to show a procedure of analysis based exclusively on the simulation results, enriching the corresponding environment, implementing a complete system.

The biggest gain values of the simulated SACM and MSACM cases generally correspond to the antenna located on the center of the roof, but

for aerodynamic behavior it is generally located on the rear part, and sometimes on the trunk. The modeling detail could be further improved, but this would increase the computer memory requirements accordingly.

The antenna performance in the reception-transmission tests shows an enough bandwidth to operate at the GPS frequency range. It was also probed that the maximum peak was very near to the designed frequency (1.57 GHz). The lightly variation can be attributed to the fabrication process. The variations in the pattern distortion of the antenna using an acrylic radome were shown. Additionally, it was possible to appreciate that the chassis contributes notably to increase the antenna gain. With the average values of the experimental tests using the GPS kit in fixed points, it can be concluded that the prototype has an adequate response as a replacement antenna, although the original antenna has a low noise amplifier.

In practical measurements on a vehicle, the result were also satisfactory, because all measured points correspond to the university circuit, as it was noted in the sampling points located using Google Maps. Some improvements could be also realized, such as: the antenna size (using alternative materials or geometries), the radome (making it with liquid acrylic or epoxy resin), and the car model (implementing additional elements or modifying shapes, but with the consequent increment of computer resources involved).

ACKNOWLEDGMENT

Authors want to thank to EM Software & Systems (USA) Inc., for FEKO license, and to Rogers Co. for the material donation for the realization of this work.

J. G. Vera-Dimas expresses his sincere thanks to CONACyT for the postgraduate scholarship under grant 270210/219230.

REFERENCES

[1] J. R. Ojha, R. Marklein, and I. Widjaja, *Technological Trends of Antennas in Cars, Advances in Vehicular Networking Technologies*, Dr. Miguel Almeida (Ed.), ISBN: 978-953-307-241-8, InTech. 2011.

[2] R. Garg, P. Bhartia, I. Bahal, and A. Ittipiboon, *Microstrip Antenna Design Handbook*, Artech House, MA, 2001.

[3] S. Nair, *A Multiple Antenna Global Positioning System Configuration for Enhanced Performance*, Thesis for the degree of Master in science, Ohio University, June 2004.

[4] http://tuning.deautomoviles.com.ar/articulos/accesorios/tecnologicos/navegadores-gps.html, Sep. 2010.

[5] http://www.aciem.org/bancoconocimiento/v/vehiculosgps/vehiculos%20gps.pdf, Sep. 2010.

[6] L. E. Frenzel, *Sistemas Electrónicos de Comunicación*, Alfaomega, México 2003.

[7] http://www.grupodeca.com.mx/productos-servicios / localizacion-automatica-vehiculos-gps/, Oct. 2010.

[8] Y. Kim, *Development of Automobile Antenna Design and Optimization for FM/GPS/SDARS Applications*, Ph.D. Dissertation, The Ohio State University, 2003.

[9] S. Alba, *Design and Performance of a Robust GPS/INS Attitude System for Automobile Applications*, Ph.D. Dissertation, Stanford University, 2004.

[10] Official U. S. Government information about the Global Positioning System (GPS) and related topics. Available at: http://www.gps.gov/systems/gps/modernization/civilsignals/, April 2013.

[11] Comisión Federal de Telecomunicaciones. *Cuadro Nacional de Frecuencias. Clasificación de Servicios* 2007.

[12] K. Yegin, "On-vehicle GPS antenna measurements," *IEEE Antennas and Wireless Propagation Letters*, vol. 6, pp. 488-491, 2007.

[13] *Engineering Notes*: OncoreTM Active Antenna, http://www. Oncore.motorola.com (April 2012).

[14] http://www.gpsenlinea.com/Vehiculos.html, Oct. 2010.

[15] J. Á. Abellán, *GNSS Array: Diseño de una Antenna con Polarización Circular*, Enginyeria de Telecomunicació. Projecte Fi de Carrera, 2009

[16] S. Murugan and V. Rajamani. "Design of wideband circularly polarized capacitive fed microstrip antenna," *International Conference on Communication Technology and System Design,* vol. 30, pp. 372-379, 2011.

[17] K. Wong, *Compact and Broadband Microstrip Antennas*, Wiley Interscience, New York, 2002.

[18] A. Rasku, *Multi-Antenna Solutions for Automotive Environment*, Master of Science Thesis, Tampere University of Technology, Nov. 2008.

[19] T. Karacolak and E. Topsakal, "Mixed order tangential vector finite elements (TVFEs) for tetrahedral and applications to multi-functional automotive antenna design," *Applied Computational Electromagnetics Society ACES Journal*, vol. 22, no. 1, pp. 117-124, 2007.

[20] M. Tecpoyotl-Torres, J. G. Vera-Dimas, R. Vargas-Bernal, M. Torres-Cisneros, A. Zamudio-

Lara, and V. Grimalsky, "Pentagonal microstrip antenna equivalent to a circular microstrip antenna for GPS operation frequency," *Memorias del 7º Congreso Internacional de Cómputo en Optimización y Software, CICOS 09*, pp. 200-208, 2009.

[21] R. H. Garg, *Microstrip Antenna Design Handbook*, Artech House, ISBN: 0-89006-513-6, 2001.

[22] J. Hong and M. J. Lancaster, *Microstrip Filters for RF/Microwave Applications*, Wiley Series in Microwave an Optical Engineering, New York, 2001.

[23] J. G. Vera-Dimas and M. Tecpoyotl-Torres, "Kit educativo para la comprensión de la propagación de ondas electromagnéticas," Memoria Técnica *ROC&C 2009. Vigésima Reunión de Otoño de Comunicaciones, Computación, Electrónica y Exposición Industrial*. Acapulco, México, 2009.

[24] http://www.audi.es/es/brand/es/Modelos/R8/r8_coupe/caracteristicas/Datos_tecnicos/Dimensiones.html, June 2012.

[25] C. A. Balanis *Antenna Theory*, 3rd edition, Wiley-Inter Science, 2005.

Margarita Tecpoyotl Torres received the Mathematician degree from the Autonomous University of Puebla (UAP), Mexico, in 1991, and the Diploma of Electronic Engineer in 1993. She received the M.Sc. and Ph.D. degrees in Electronics from INAOE, in 1997 and 1999, respectively. Dr. Tecpoyotl works, since 1999, at CIICAp of the UAEM, Mexico, where she is currently titular Professor. Her main research interest includes MEMS, antenna design, and microwave devices. She has currently two patents, conceded by Mexican Institute of Intellectual Property, IMPI, and other two under revision. She holds the status of National Researcher (SNI) level 1.

José Gerardo Vera Dimas graduated from the Technologic of Morelia as Electronic Engineer. Member IEEE since January 2005. Commit member of VII and VIII ROPEC. He received the award of "EGRETEC 2009" by the Association of Graduates from the Technological Institute of Morelia. He received the M.Sc. degree in Electronics from UAEM. Nowadays, he is a Ph. D. degree student in CIICAp at UAEM. He has currently two patents in revision.